

A Versatile Method for Tuning the Chemistry and Size of Nanoscopic Features by Living Free Radical Polymerization

Timothy A. von Werne,[†] David S. Germack,[†] Erik C. Hagberg,[‡] Valerie V. Sheares,[‡] Craig J. Hawker,^{*,†} and Kenneth R. Carter^{*,†}

Contribution from the IBM Almaden Research Center, Center for Polymeric Interfaces and Macromolecular Assemblies, 650 Harry Road, San Jose, California 95120-6099, and Department of Chemistry, Iowa State University, Ames, Iowa 50011

Received October 8, 2002; E-mail: hawker@almaden.ibm.com; krcarter@almaden.ibm.com

Abstract: A novel approach is presented for manipulating the size and chemistry of nanoscopic features using a combination of contact molding and living free radical polymerization. In this approach a highly cross-linked photopolymer, based on a methacrylate/acrylate mixture, was patterned into submicrometer-sized features on a silicon wafer using a contact-molding technique. A critical component of the monomer mixture was the incorporation of an initiator containing monomer into the network structure, which provides sites for functional group amplification. Features ranging in size from 5 μm to <60 nm were accurately replicated by this process and living free radical polymerizations, both atom transfer radical and nitroxide-mediated polymerization (NMP), could be conducted from these initiating sites to yield polymer brushes which represent a grafted layer of linear chains attached to the original network polymer. Grafts consisting of polystyrene, poly(methyl methacrylate), and poly(2-hydroxyethyl) methacrylate were grown with controlled thicknesses ranging from 10 to 143 nm and graft molecular weights of between 18 000 to 290 000 amu. As a result of this secondary graft process, feature sizes could be tuned from the original 100 nm down to 20 nm, and the surface chemistry varied from hydrophilic to hydrophobic starting from the same initial master pattern. The thin films and patterned features were characterized by contact angle, ellipsometry, optical, and atomic force microscopies.

Introduction

The fabrication of nanometer-sized structures and devices is an area of increasing importance due to its commercial importance and application to the emerging field of nanoscale science. Advances in the fields of molecular-scale electronics, magnetic storage, optoelectronics, and biotechnology all depend increasingly on the ability to fashion materials with precise control of feature size and functionality.¹ The fabrication techniques have largely been split into two broad categories, namely “top-down” approaches and “bottom-up” approaches. Classical top-down processes include well-known microfabrication techniques such as photolithography^{2–4} which is currently used to make essentially all modern microelectronic devices. Bottom-up approaches are more dependent on the chemistry and functionality of the materials employed and includes the use of self-organizing materials that can undergo pattern formation at nanoscale levels to give technologically interesting structures.^{5,6} Both strategies for the fabrication of nanoscale

structures have their own unique advantages and drawbacks. For example, top-down approaches are well understood, reproducible and scaleable, although advances become more difficult as device features drop below the 100-nm level. In contrast, bottom-up approaches show promise in the ability to make sub-100 nm features, but thus far the ability to utilize bottom-up approaches to fashion useful devices of known architecture has proven elusive due to the inherent difficulty of directing the exact positioning of self-assembling systems over large areas.

In an attempt to fabricate sub-100 nm nanostructures, especially in the microelectronics arena, researchers have concentrated on the patterning of thin organic films, which in turn are utilized as masks or resist materials for other secondary fabrication processes. Reported methods for the synthesis of nanoscopically patterned thin organic films include state-of-the-art photolithographic techniques, advanced lithographic techniques such as e-beam patterning, and other nonoptical contact patterning techniques. These contact lithographic techniques include nanoimprint lithography,⁷ “step and flash”

[†] IBM Almaden Research Center.

[‡] Iowa State University.

- (1) (a) Mirkin, C. A.; Rogers, J. A. *MRS Bull.* **2001**, 26, 506. (b) Russell, T. P. *Science* **2002**, 297, 964.
- (2) Klopp, J. M.; Pasini, D.; Byers, J. D.; Willson, C. G.; Frechet, J. M. J. *Chem. Mater.* **2001**, 13, 4147.
- (3) Tully, D. C.; Trimble, A. R.; Frechet, J. M. J. *Adv. Mater.* **2000**, 12, 1118.
- (4) Tran, H. V.; Hung, R. J.; Chiba, T.; Yamada, S.; Mrozek, T.; Hsieh, Y. T.; Chambers, C. R.; Osborn, B. P.; Tringue, B. C.; Pinnow, M. J.; MacDonald, S. A.; Willson, C. G.; Sanders, D. P.; Connor, E. F.; Grubbs, R. H.; Conley, W. *Macromolecules* **2002**, 35, 6539.

- (5) (a) Ma, Q. G.; Remsen, E. E.; Kowalewski, T.; Wooley, K. L. *J. Am. Chem. Soc.* **2001**, 123, 4627. (b) Thurn-Albrecht, T.; Schotter, J.; Kastle, C. A.; Emley, N.; Shibauchi, T.; Krusin-Elbaum, L.; Guarini, K.; Black, C. T.; Tuominen, M. T.; Russell, T. P. *Science* **2000**, 290, 2126.
- (6) Quite often discussions concerning bottom-up approaches have been dominated by self-assembly of molecules and nano-objects through noncovalent interactions. The polymerization of monomers directed to prepatterned areas can also be considered a bottom-up approach, albeit different from materials that self-organize at surfaces.
- (7) Chou, S. Y.; Krauss, P. R.; Renstrom, P. J. *J. Vac. Sci. Technol., B* **1996**, 14, 4129.

imprint lithography,⁸ nanocontact molding,⁹ and derivations of the above-mentioned microcontact printing of self-assembled monolayers (SAMs). A recent report demonstrated the construction of <30-nm structures by a “molecular ruler” approach.¹⁰ In that work, metal lines were patterned by e-beam lithography techniques followed by alteration of the pattern size by adsorbing organic monolayers on the metal surfaces. Then a second metal layer was deposited over the size-adjusted features, followed by lift-off of the organic layer. Fabrication of metallic features smaller than 30 nm was demonstrated by using this novel process. While other research groups working in imprint lithography have mainly focused on improving the physics of the imprint process, we have concentrated on novel polymeric materials used in the process, specifically to improve control of the size and functionality of nanometer-sized features.

In concert with these advances, one bottom-up approach, which has received considerable attention in recent years, is the controlled growth of polymer brushes from surface-initiated sites. This affords polymer brushes of well-defined nanoscopic structure, molecular weight, and controllable molecular architecture, which have found application in a variety of different areas. A number of surface-bound “living” polymerization initiators including cationic,¹¹ anionic,¹² ring-opening,¹³ ATRP,^{14–18} TEMPO,¹⁹ and RAFT^{20,21} have been successfully employed to give surface-grafted polymers under controlled growth conditions. Several researchers have improved upon this technique by patterning the initiator on the surface by microcontact printing techniques followed by controlled polymerization to yield surfaces decorated with patterned surface-tethered polymers.^{22,23} These patterning techniques have potential applications in creation of microstructures, but there are several limitations inherent with PDMS-based microcontact printing, namely poor monolayer coverage, limitations in resolution, and lack of robustness of adsorbed initiator monolayers. Polymers demonstrated as “inking” stamps for use in microprinting techniques are generally based on PDMS, which does not easily replicate nanometer-sized features due to its inherently low modulus and the tendency for small structures to collapse under the forces of self-adhesion. Additionally, PDMS readily deforms under applied pressure, making alignment and controlled contact over large areas a continued challenge.

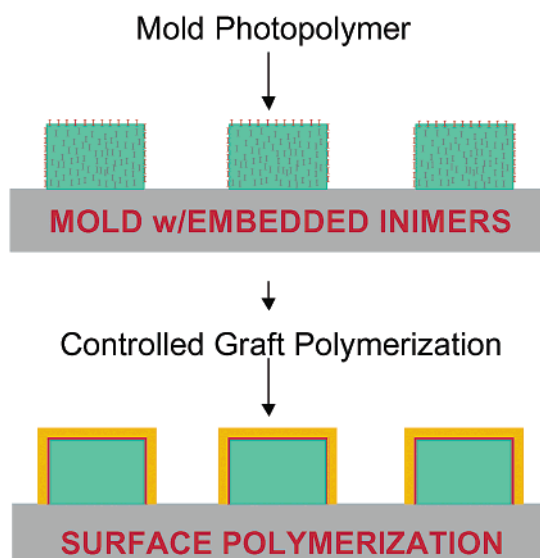


Figure 1. Graphical representation of surface tuning for nanoscopic pattern replication.

Herein we report a new tandem, top-down/bottom-up approach for controlling the chemistry and size of nanoscopic features at the sub-100 nm level, which is both simple and versatile (Figure 1). In this strategy, a top-down nanocontact-molding process is employed followed by the controlled growth of polymer brushes from these patterned features (bottom-up). This is achieved by molding a network photopolymer, containing an imbedded inimer (having both an *initiator* and *monomer* fragment²⁴), into patterned features. In a secondary reaction step, polymer brushes of defined chemistry and structure are grown from the surface of the patterned network, specifically from the exposed imbedded inimers, thus changing the size of the features and the surface chemistry of the features. As a consequence of this strategy, a variety of nanoscopic structures with different feature sizes and functional groups can be grown from the same, original molded template.

Experimental Section

Materials. Unless specified, all reagents were used without further purification. Styrene, methyl methacrylate (MMA), and 2-hydroxyethyl methacrylate (HEMA) from Aldrich were dried over CaH₂ and distilled under reduced pressure. Ethoxylated bisphenol A dimethacrylate (Sartomer), *N*-vinyl pyrrolidone (Aldrich) and 2-ethyl-2-(hydroxymethyl)-1,3-propanediol trimethacrylate (TMPA) (Aldrich) were used as received. 2,2-Dimethoxy-2-phenylacetophenone (DMPA) was recrystallized prior to use. 3-Methacryloxypropyl trichlorosilane was used as received from UCT. All reactions were run under dry N₂ unless otherwise noted. Patterned silicon masters were supplied by SEMATECH or made by e-beam lithography. We used electronic grade propylene glycol methyl ether acetate (PGMEA) to make solutions for the thin film photopolymer resins.

Instrumentation. Gel permeation chromatography (GPC) was performed on a Waters chromatograph (four Waters Styragel HR columns HR1, HR2, HR4, and HR5E in series) connected to a Waters 410 differential refractometer with THF as the eluent. Molecular weight standards were narrow polydispersity polystyrenes. Ellipsometry was carried out on a Rudolph Auto-EI ellipsometer. Contact angle measurements were recorded on a VCA 2500 video contact angle system with a drop size of 1.00 μ L. Electron micrographs were recorded on a Hitachi S-4700 scanning electron microscope (SEM). AFM micrographs were

- (8) Bailey, T.; Choi, B. J.; Colburn, M.; Meissl, M.; Shaya, S.; Ekerdt, J. G.; Sreenivasan, S. V.; Willson, C. G. *J. Vac. Sci. Technol., B* **2000**, *18*, 3572.
- (9) McClelland, G. M.; Hart, M. W.; Rettner, C. T.; Best, M. E.; Carter, K. R.; Terris, B. D. *J. Appl. Phys. Lett.* **2002**, *81*, 1483.
- (10) Hatzor, A.; Weiss, P. S. *Science* **2001**, *291*, 1019.
- (11) Jordan, R.; Ulman, A. *J. Am. Chem. Soc.* **1998**, *120*, 243.
- (12) Jordan, R.; Ulman, A.; Kang, J. F.; Rafailovich, M. H. *J. Am. Chem. Soc.* **1999**, *121*, 1016.
- (13) Weck, M.; Jackiw, J. J.; Rossi, R. R.; Weiss, P. S.; Grubbs, R. H. *J. Am. Chem. Soc.* **1999**, *121*, 4088.
- (14) Boyes, S. G.; Brittain, W. J.; Weng, X.; Cheng, S. Z. D. *Macromolecules* **2002**, *35*, 4960.
- (15) von Werne, T. A.; Patten, T. E. *J. Am. Chem. Soc.* **2001**, *123*, 7497.
- (16) Boerner, H. G.; Duran, D.; Matyjaszewski, K.; da Silva, M.; Sheiko, S. S. *Macromolecules* **2002**, *35*, 3387.
- (17) Ejaz, M.; Yamamoto, S.; Ohne, K.; Tsujii, Y.; Fukuda, T. *Macromolecules* **1998**, *31*, 5934.
- (18) Huang, X.; Wirth, M. J. *Macromolecules* **1999**, *32*, 1694.
- (19) Husemann, M.; Malmstrom, E.; McNamara, M.; Mate, M.; Mecerreyes, D.; Benoit, D.; Hedrick, J.; Mansky, P.; Huang, E.; Russell, T.; Hawker, C. J. *Macromolecules* **1999**, *32*, 1424.
- (20) De Boer, B.; Simon, H. K.; Werts, M. P. L.; van der Vegte, E. W.; Hadziioannou, G. *Macromolecules* **2000**, *33*, 349.
- (21) Luo, N.; Hutchinson, J. B.; Anseth, K. S.; Bowman, C. N. *J. Polym. Sci., Part A: Polym. Chem.* **2002**, *40*, 1885.
- (22) Husemann, M.; Mecerreyes, D.; Hawker, C. J.; Hedrick, J. L.; Shah, R.; Abbott, N. L. *Angew. Chem., Int. Ed.* **1999**, *38*, 647.
- (23) Jones, D. M.; Huck, W. S. *Adv. Mater.* **2001**, *16*, 1256.

- (24) Mueller, A. H. E.; Yan, D.; Wulkow, M. *Macromolecules* **1997**, *30*, 7015.

recorded in tapping mode on a Nanoscope III from Digital Instruments. FTIR spectra were recorded in transmission mode on a Thermo NicoletNexus 670 FTIR spectrometer using double polished wedged silicon wafers.

Photopolymer Solution. The base photopolymer solution (PPI) consisted of the following formulation: ethoxylated bisphenol A dimethacrylate (61%), *N*-vinyl pyrrolidone (18.5%), 2-ethyl-2-(hydroxymethyl)-1,3-propanediol trimethacrylate (18.5%), and 2,2-dimethoxy-2-phenylacetophenone (2%). The monomers and initiator were mixed and stored refrigerated in the dark prior to use.

Synthesis of 2-Methacryloxyethyl-2'-bromoisobutyrate (IN-1). A three neck flask containing 200 mL of dry THF, 4.24 g (32.6 mmol) of 2-hydroxyethyl methacrylate, and 3.30 g (32.6 mmol) of triethylamine was equipped with a stir bar and cooled to 0 °C in an ice bath. Using an addition funnel, 8.74 g (38.0 mmol) of 2-bromoisobutryl bromide was added dropwise. Upon complete addition, the mixture was brought to room temperature and allowed to stir for 18 h. The product was washed with 3 × 100 mL of H₂O and dried over anhydrous MgSO₄, and the solvent was evaporated. The remaining pale yellow oil was distilled under reduced pressure (200 mTorr) at 75 °C, and 5.94 g (65.2%) of the product, **IN-1**, was collected. ¹H NMR (250 MHz, CDCl₃) δ (ppm) 6.07 (1H, s), 5.53 (1H, s), 4.13 (4H, s), 1.94 (6H, d), 1.86 (3H, s). ¹³C {¹H} NMR (62.5 MHz, CDCl₃) δ (ppm) 170.2, 135.8, 126.1, 63.4, 61.9, 55.3, 30.6, 18.2. Anal. Calcd for C₁₀H₁₅BrO₄: C, 43.0; H, 5.42. Found: C, 42.8; H, 5.64.

Synthesis of 2,2,5-Trimethyl-3-(1'-(4'-acetoxyl)phenylethoxy)-4-phenyl-3-azahexane, 2. In 34.3 mL of hexamethylphosphoramide (HMPA) was dissolved 8.58 g (23.0 mmol) of 2,2,5-trimethyl-3-(1-(4-chloromethyl)phenylethoxy)-4-phenyl-3-azahexane, **1**.²⁵ To this was added 6.74 g (68.7 mmol) of potassium acetate, and the mixture was stirred for 2 days at room temperature. The reaction mixture was then loaded onto a silica gel flash column with hexane as the solvent. After 500 mL of hexane was run through the column to remove the HMPA, the product was separated from the starting material by eluting with a 1:1 mixture of hexane and methylene chloride. The solvent was removed in vacuo to give the acetoxyl derivative, **2**, as a thick, clear yellow oil, 8.51 g (93.0%); ¹H NMR both diastereomers (250 MHz, CDCl₃) δ 7.10–7.40 (m, 18H), 5.12 (d, 2H, *J* = 9.3 Hz), 4.91 (ds, 4H, *J* = 3.2 Hz), 3.45 (d, 1H, *J* = 10.8 Hz), 3.31 (d, 1H, *J* = 10.8 Hz), 2.44 (m, 1H), 1.60 (d, 3H *J* = 6.3 Hz), 1.52 (d, 3H *J* = 6.3 Hz), 1.41 (m, 1H), 1.28 (d, 3H, *J* = 6.3 Hz), 1.07 (s, 9H), 0.88 (d, 3H *J* = 6.3 Hz), 0.81 (s, 9H), 0.60 (d, 3H, *J* = 6.6 Hz), 0.21 (d, 3H *J* = 6.6 Hz); ¹³C NMR (APT) (63 MHz, CDCl₃, both diastereomers) δ 172.54 (s), 146.03 (s), 145.27 (s), 142.80 (s), 142.35 (s), 135.78 (d), 131.04 (d), 128.51 (d), 127.36 (d), 127.31 (d), 127.19 (d), 127.05 (d), 126.50 (d), 126.37 (d), 126.23 (d), 83.23 (d), 82.30 (d), 72.12 (d), 72.10 (d), 63.20 (t), 60.55 (s), 60.48 (s), 46.20 (d), 32.07 (d), 31.77 (d), 28.45 (q), 28.23 (q), 25.48 (q), 24.70 (q), 23.08 (q), 23.01 (q), 22.12 (q), 21.30 (q), 21.19 (q). Anal. Calcd for C₂₅H₃₅NO₃: C, 75.5; H, 8.87; N, 3.52. Found: C, 75.3; H, 8.82; N, 3.70.

Synthesis of 2,2,5-Trimethyl-3-(1'-(4'-hydroxymethyl)phenylethoxy)-4-phenyl-3-azahexane, 3. In 100 mL of a 3:1 mixture of water/ethanol was dissolved 8.5 g (21 mmol) of the acetoxyl derivative, **2**. Potassium hydroxide (3.4 g, 61 mmol) was added, and the mixture was heated to reflux with stirring. Once the reaction was refluxing a small amount of ethanol (ca. 10 mL) was added to afford a clear, single-phase reaction mixture. After 2 h at reflux the reaction was allowed to cool to room temperature and extracted four times with 80 mL of methylene chloride and then dried over magnesium sulfate. The solvent was removed in vacuo, and the product was separated from starting materials on a silica gel flash column, eluting with a 1:1 mixture of methylene chloride/hexane going to pure methylene chloride to give the desired hydroxy functionalized alkoxyamine, **3**, 4.63 g (61% yield).

¹H NMR both diastereomers (250 MHz, CDCl₃) δ 7.10–7.40 (m, 18H), 4.96 (m, 2H), 4.74 (m, 4H), 3.40 (d, 1H, *J* = 10.8 Hz), 3.31 (d, 1H, *J* = 10.8 Hz), 2.42 (m, 1H), 1.59 (d, 3H *J* = 6.3 Hz), 1.50 (d, 3H *J* = 6.3 Hz), 1.41 (m, 1H), 1.32 (d, 3H, *J* = 6.3 Hz), 1.05 (s, 9H), 0.93 (d, 3H *J* = 6.3 Hz), 0.78 (s, 9H), 0.61 (d, 3H, *J* = 6.6 Hz), 0.19 (d, 3H *J* = 6.6 Hz); ¹³C NMR (APT) (63 MHz, CDCl₃, both diastereomers) δ 146.11 (s), 145.24 (s), 142.55 (s), 135.67(d), 131.12 (d), 128.43 (d), 127.33 (d), 127.16 (d), 127.03 (d), 126.42 (d), 126.21 (d), 83.19 (d), 82.34 (d), 72.10 (d), 63.05 (t), 60.68 (s), 60.52 (s), 32.17 (d), 31.70 (d), 28.50 (q), 28.24 (q), 24.73 (q), 23.09 (q), 22.10 (q), 21.19 (q). Anal. Calcd for C₂₅H₃₃NO₂: C, 77.7; H, 9.35; N, 3.94. Found: C, 77.6; H, 9.13; N, 3.68.

Synthesis of 2,2,5-Trimethyl-3-(1'-(4'-methacryloyloxymethyl)phenylethoxy)-4-phenyl-3-azahexane, IN-2. In 20 mL of dry THF in a three-neck flask equipped with a reflux condenser, rubber septa, and N₂ bubbler was dissolved 2.01 g (5.66 mmol) of the hydroxy derivative, **3**. Dry triethylamine, 1.51 mL (10.8 mmol) was added with stirring followed by the dropwise addition of methacryloyl chloride, 1.4 mL (14.5 mmol). The reaction was allowed to stir at room temperature for 2.5 h, and then 50 mL of methylene chloride was added; the mixture was washed three times with 100 mL of water. The organic layers were combined and reduced in volume in vacuo to about 4 mL of crude product. The product was washed again with two aliquots of 10% NaOH and 10% HCl and then run through a silica gel flash column with 95% hexane, 5% ethyl acetate to yield 1.53 g (65.9% yield). ¹H NMR (250 MHz, CDCl₃) δ 7.3–6.8 (m, 9H), 5.9 (1H, s), 5.4 (1H, s), 5.1 (1H, s), 5–4.9 (2H, d), 4.8–4.6 (1H, m), 3.3–3 (1H, m), 1.8 (3H, s), 1.5–1.2 (4H, m), 1.1 (2H, d), 0.8 (4H, s), 0.7 (2H, d), 0.6 (4H, s), 0.3 (1H, d), 0.1 (1H, d). ¹³C {¹H} NMR (62.5 MHz, CDCl₃) δ 166.4, 146.3, 145.6, 142.7 (d) 135.3, 134.6, 131.4, 128.7, 127.7 (t), 126.7 (t), 83.7, 82.8, 72.6, 66.6, 60.9, 32.5, 32.1, 28.8, 25.2, 23.6, 23.1, 22.5, 21.6, 14.6. Anal. Calcd for C₂₇H₃₇NO₃: C, 76.6; H, 8.80; N, 3.31. Found: C, 76.4; H, 8.92; N, 3.45.

Silicon Wafer Preparation. Polished silicon wafers were soaked in a concentrated sulfuric acid solution containing *No-Chromix* for 5 min and rinsed extensively with deionized water. The wafers were then placed in a 2-propanol vapor bath for 5 min and dried in an oven. An adhesion promoter, 3-methacryloxypropyl trichlorosilane, was then vapor-deposited on the silicon wafer under a saturated stream of dry nitrogen.

Mold Fabrication. Patterned silicon masters with the desired features to be replicated were cleaned as described above. A thin (150 nm) glass plate was cleaned using the same procedure used above and exposed to 3-methacryloxypropyl trichlorosilane vapor for 5 min to form an adhesion layer. A small amount of PPI resin (0.1 mL) was added to the surface of the silicon master, and the glass plate was brought into contact. The viscous liquid was allowed to spread between the two plates and then exposed at 365-nm light (14 mW/cm²) for 1 min. The glass plate was carefully separated from the silicon master, yielding a patterned PPI network mold on a thin glass backing plate. This mold was then sputter-coated with a 2–4-nm thick layer of Au/Pd alloy and stored under nitrogen.

Pattern Transfer. The photopolymer used for the replica layer in contact patterning consisted of PPI doped with 10–20 wt % of the desired inimer, **IN-1** or **IN-2**. This doped mixture was then diluted with propylene glycol methyl ether acetate (PGMEA) to yield a 3 wt % solution. This solution was filtered onto a cleaned and prepared silicon wafer and spun at 3000 rpm for 1 min, yielding a 30-nm-thick film. The Au/Pd coated mold was brought into contact with the wafer, and a pressure of 60 psi was applied. The wafer was exposed using 365-nm light (14 mW/cm²) for 1 min, and then the mold was peeled off leaving an inimer-embedded network replica layer on the surface of the wafer. Additional information on the contact-molding process used can be found in our earlier reference.⁹

Styrene Graft ATRP from Inimer-Embedded Network Thin Film. A silicon wafer coated with a cured thin film network consisting

(25) Benoit, D.; Chaplinski, V.; Braslau, R.; Hawker, C. J. *J. Am. Chem. Soc.* **1999**, *121*, 3904.

of PP1 doped with 10 wt % ATRP inimer (IN-1), was added to a Schlenk flask containing 10.2 mg (7.1×10^{-5} mol) of CuBr and a stir bar. Styrene (2.50 mL, 21.8 mmol), pentamethyldiethylenetriamine (PMDETA) (13.0 μ L, 7.0×10^{-5} mol), and ethyl-2-bromoisobutyrate (4.0 μ L, 2.2×10^{-5} mol) were added via syringe, and 2.5 mL of *p*-xylene was added as a solvent. The flask was purged of oxygen via three cycles of freeze, pump, thaw, and backfilling with N₂. The reaction was sealed and heated at 90 °C for 4 h and then cooled. The wafer was removed from the flask and rinsed liberally with acetone and THF. Any physisorbed polymer was removed by exhaustive extraction with THF in a Soxhlet apparatus.

MMA Graft ATRP from Inimer-Embedded Network Thin Film. MMA polymerizations were performed as reported for styrene with the exception that 2.50 mL (22.2 mmol) of MMA was substituted for styrene and the polymerization was conducted at 60 °C for 4 h.

HEMA Graft ATRP from Inimer-Embedded Network Thin Film.²⁶ A silicon wafer coated with a cured thin film network consisting of PP1 doped with 10 wt % ATRP inimer (IN-1), was added to a Schlenk flask containing 10.2 mg (7.1×10^{-5} mol) of CuBr and a stir bar, and the flask was deoxygenated by purging with N₂. In a 10-mL round-bottom flask, CuBr (9.0 mg, 6.3×10^{-5} mol), dipyriddy (14.0 mg, 1.2×10^{-4} mol), and HEMA (1.5 mL, 10.8 mmol) were added followed by 1.0 mL of H₂O and 2.5 mL of methanol as solvents, and the reaction mixture purged with N₂. The contents of the round-bottom flask were added to a Schlenk flask via a purged syringe, and the polymerization was left to stir at room temperature for 4 h, after which time the wafer was removed and rinsed liberally with acetone and methanol.

Alkoxyamine Initiated Graft Polymerization from Inimer-Embedded Network Thin Film. A silicon wafer coated with a cured thin film network consisting of PP1 doped with 10 wt % alkoxyamine-based inimer (IN-2) was added to a Schlenk flask containing styrene (3.0 mL, 26.2 mmol), free alkoxyamine initiator (0.80 mg, 0.0023 mmol), and chlorobenzene as a solvent (2.0 mL). A stir bar was added, and the flask was deoxygenated via three cycles of freeze, pump, thaw, and backfilling with N₂. The flask was sealed and heated at 125 °C for 16 h, after which time the wafer was removed and rinsed liberally with THF and acetone.

Results and Discussion

The primary patterning technique used in this approach is a top-down contact-molding process which involves the use of a patterned polymeric mold to template a secondary liquid photopolymer resin layer that is subsequently UV-polymerized while in contact with the mold to give pattern transfer (Figure 2).⁸ The patterned polymeric mold is formed by casting a photopolymer resin (PP1) on a hard master, in our case either SiO₂ or Si, and photopolymerizing the resin to give a polymeric network mold that has negative features of the original master. Many molds can be made from a single master, and subsequently many imprints can be made from a single mold. As a consequence, this process allows low throughput, high-cost lithographic methods, such as electron beam and X-ray lithography, to be used to fabricate a single master, which can then be reproduced to fabricate many replicas. The composition of the PP1 resin formulation was optimized for a number of criteria including network hardness after cure, shrinkage, cure rate, and UV absorption.⁹ The optimal composition is shown in Scheme 1.

The ethoxylated bisphenol A dimethacrylate imparts hardness, etch resistance, and rigidity. The trimethacrylate provides a high

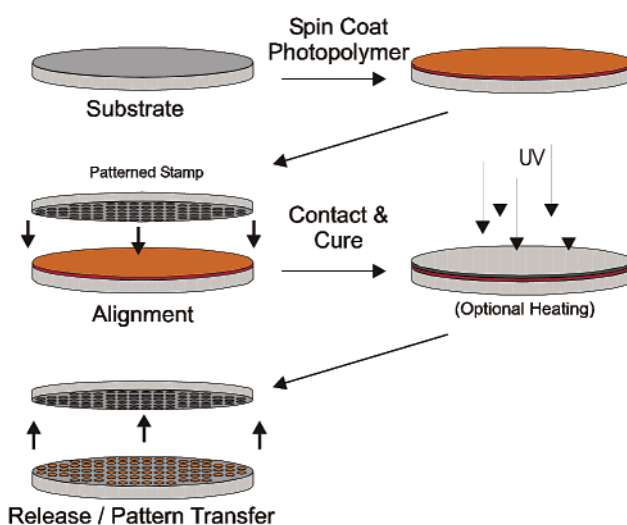
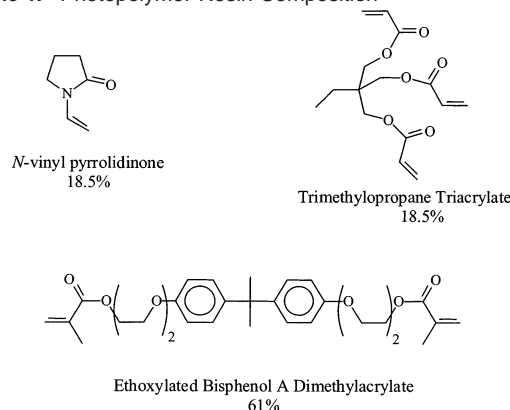


Figure 2. Representation of contact-molding process.

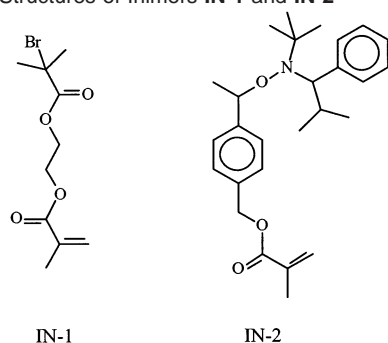
Scheme 1. Photopolymer Resin Composition



cross-linking density, and the *N*-vinyl pyrrolidone serves to increase chain propagation rates during cure when using 2,2-dimethoxy-2-phenylacetophenone (DMPA) as a photoinitiator at 365 nm.

The contact-molding process required the availability high-quality patterned masters. For our initial experiments the master consisted of etched silicon wafers with test features ranging from 5.0 to 0.35 μ m, with a feature depth of 1.0 μ m. To make the reusable mold for the replication process, the PP1 resin mixture was applied to the surface of the master, and a thin glass backing plate was brought into contact with the resin, forming a sandwich structure. The PP1 was cured under UV light, and after curing, the mold on the backing plate was carefully removed from the silicon master. The glass backing plate had been treated with an adhesion promoter to ensure the cured network polymer layer would have good adhesion to the glass versus the Au/Pd coated master. The polymer network mold represented a negative relief image of the silicon master. This mold was then coated with a thin (2–4 nm) layer of Au/Pd to prevent subsequent adhesion of the mold to any photopolymer resin layers during pattern replication. The network polymer mold on the glass backing plate was then used to replicate the desired pattern into a second photopolymer layer by contact molding. The photopolymer resin PP1 was diluted to 3 wt % in PGMEA and spin-coated onto a silicon wafer that had been cleaned and treated with adhesion promoter. The mold was brought into contact with the thin film photopolymer resin on

(26) Fuji, Y.; Watanabe, K.; Baek, K.-Y.; Ando, T.; Kamigaito, M.; Sawamoto, M. *J. Polym. Sci., Part A: Polym. Chem.* **2002**, *40*, 2055–2065.

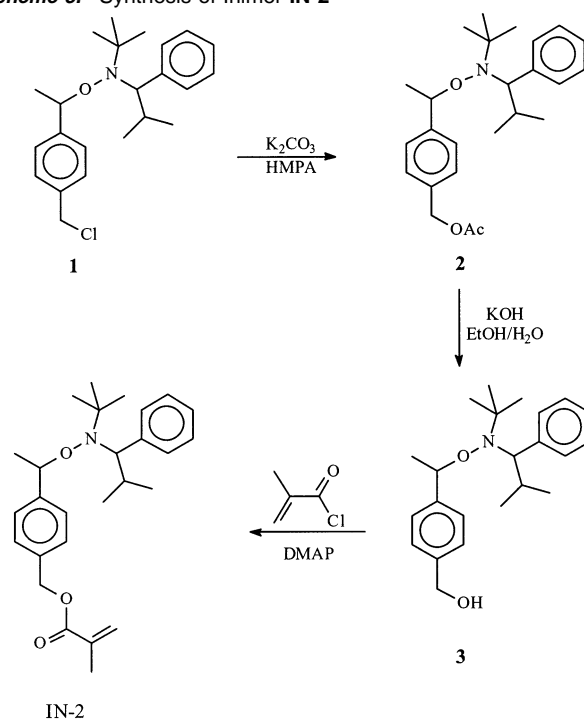
Scheme 2. Structures of Inimers **IN-1** and **IN-2**

the wafer, pressure (60 psi) was applied, and the mold/photopolymer/wafer sandwich was exposed to UV light. After the photocure, the mold was released to yield a positive image of the original pattern in the cured thin photopolymer on the wafer. If necessary, any residual polymer remaining in the flat areas between the molded features was removed using a descumming process, such as dry plasma etching.

To allow controlled graft polymerization from the surface-molded polymer networks, functionalized methacrylate monomers containing a dormant living free radical initiator, termed inimers (*initiators-/monomers*), were added to the **PP1** photopolymer resin mixture. This resulted in the embedded inimers being covalently bound throughout the cross-linked polymer network, with a certain fraction of those groups being advantageously located at the surface of the network and available for subsequent reactions. The inimers utilized in this study, **IN-1** and **IN-2**, are shown in Scheme 2 and are based on either atom transfer radical polymerization (ATRP) or NMP.

ATRP has been shown to be a facile route to well-defined polymers for a range of monomers at moderate temperatures.²⁷ Accordingly, the synthesis of 2-methacryloxyethyl-2'-bromoisobutyrate (**IN-1**) was accomplished through the coupling of 2-hydroxyethyl methacrylate (HEMA) with 2-bromoisobutyryl bromide which gives **IN-1** in 65% isolated yield after distillation. As a complement to the ATRP-based system, NMP-based procedures were also examined since it does not require the addition of a catalyst that can leave trace metals in the polymer.²⁸ The alkoxyamine-based inimer 2,2,5-trimethyl-3-(1'-(4''-methacryloylmethyl)phenylethoxy)-4-phenyl-3-azahexane, **IN-2**, was synthesized in a three-step process as shown in Scheme 3.

The successful use of the embedded inimer in this contact-molding approach relies on two critical features: (1) the ability to form stable cross-linked networks in the presence of the inimers and (2) retention of activity for the inimers after the photopolymerization process. To investigate the effect of the inimer groups on network formation, the methacrylate derivatives, 10–20 wt % of either inimer (**IN-1** or **IN-2**) were added to **PP1** resin formulations. These embedded inimer formulations were subsequently polymerized by exposure to UV radiation, and the cured cross-linked networks were observed to have no noticeable decrease in toughness or hardness, indicating that the addition of up to 20 wt % inimer does not have any detrimental effect on mold formation or mechanical properties.

Scheme 3. Synthesis of Inimer **IN-2****Table 1.** Contact Angle Measurements of Photopolymer Films

inimer	inimer wt %	monomer	water contact angle (deg)	
			initial	after polymerization
N/A	N/A	styrene	69.7	69.2
ATRP	20	HEMA	68.6	44.5
ATRP	20	MMA	68.9	70.1
ATRP	20	styrene	69.2	87.6
NMP	20	styrene	69.3	96.1

It is however presumed that the inimer molecules are well dispersed throughout the entire cured resin with a fraction of them advantageously located at or near the surface being accessible for subsequent “living” graft polymerizations.

The stability of the inimers to the photopolymerization process was then probed by studying the growth of polymer brushes from inimer-embedded networks. In this case thin films with no patterns (i.e., flat) were initially used since this allows for the investigation of surface characteristics and polymer growth by changes in film thickness and contact angle measurements. These flat surfaces were prepared by molding thin films of the photopolymer resin while in contact with a mold that consisted of a flat, polished silicon wafer. In addition to inimer-embedded thin films, we routinely prepared undoped networks of cured **PP1** to be used as control specimens. All of the films were characterized using water contact angle measurements to investigate the surface properties of the films and ellipsometry to determine the thickness of the thin films. Table 1 shows the measured contact angle for both the films containing the embedded inimers and the control sample before and after grafting reactions. The incorporation of 20% of the ATRP-based inimer into the cross-linked photopolymer network did not have an appreciable effect on the surface energy of the thin film as no change in the contact angle was observed, all samples having a contact angle of $\sim 69^\circ$. The corresponding film thickness of the doped and the undoped films are presented in Table 2.

(27) (a) Kamigaito, M.; Ando, T.; Sawamoto, M. *Chem. Rev.* **2001**, *101*, 3689–3746. (b) Matyjaszewski, K.; Xia, J. *Chem. Rev.* **2001**, *101*, 2921–2990.
 (28) (a) Hawker, C. J.; Bosman, A. W.; Harth, E. *Chem. Rev.* **2001**, *101*, 3661–3688. (b) Hawker, C. J. *Acc. Chem. Res.*, **1997**, *30*, 373.

Table 2. Ellipsometry Film Thickness Data

inimer	inimer wt. %	monomer	film thickness (nm)		solution polymer, M_n	solution polymer, M_w/M_n
			initial	after polymerization		
N/A	N/A	styrene	26.3	26.1	N/A	N/A
ATRP	20	HEMA	26.1	39.5	N/A	N/A
ATRP	20	MMA	35.8	64.5	3.27×10^4	1.22
ATRP	20	styrene	27.9	48.2	3.10×10^4	1.12
ATRP	40	MMA	25.2	54.4	3.30×10^4	1.14
NMP	20	styrene	17.2	160	2.90×10^5	1.48

After initial surface characterization, the thin films were subjected to ATRP polymerization conditions. The polymer-coated wafers were heated in a Schlenk flask with monomer, solvent, and catalyst (when necessary) under a nitrogen atmosphere. “Sacrificial” free initiator was added to the polymerization system to ensure that a living polymerization was achieved and to control film thickness.¹⁹ After polymer brush formation, the wafers were extensively rinsed and carefully dried to ensure that any physisorbed polymer or solvent was removed from the films. This is an important step due to the presence of sacrificial initiator during the polymerization reaction, which leads to the production of nonsurface attached polymer in solution. In each case, a control wafer with a thin film of undoped **PP1** was subjected to identical ATRP conditions to determine if there was any change in the surface properties or the film thickness after being subjected to polymerization with different monomers and at different temperatures. For styrene, HEMA, and MMA under ATRP conditions and for styrene under NMP polymerization conditions at 125 °C, no change in the undoped films was observed after polymerization. Characterization data of the films before and after surface polymerization is presented in Tables 1 and 2.

For the networks that did contain embedded inimers, contact angle measurements gave a qualitative indication of significant chemical changes to the surface of the thin film and the associated growth of polymer brushes (Table 1). In the case of the wafer exposed to MMA/ATRP conditions, a contact angle of 70° was observed after surface polymerization. This represented little, if any change in the surface energy and may be expected since a MMA brush was being grafted to a methacrylate-based network. However, in the case of both the styrene and HEMA polymerizations, significant surface energy changes were noted. The film grafted with the hydrophilic HEMA brush would result in a high surface energy film and as expected the water contact angle of this sample decreased from an initial value of 69° to 45°. Conversely, grafting the more hydrophobic polystyrene brush using both ATRP and NMP techniques caused the surface energy to drop as evidenced by the increase in the water contact angle to 88° and 96° respectively. These values are in good agreement with reported contact angle measurements of 90°–96° of pure polystyrene films.²⁹ The polymer brush coverage appears to be more dense in the thicker sample as evidenced by the higher contact angle measured (48 nm and 88° for the ATRP polymerization vs 160 nm and 96° for the NMP polymerization). Repeated measurements on a number of samples over various areas of the substrate showed that uniform modification of the inimer embedded surface was achieved which demonstrates the utility of this bottom-up approach. It is

important to note that the control sample containing no embedded inimer showed no appreciable change in surface energy after ATRP polymerization. These results support the assertion that the differences in contact angle are due to actual modification of the surface and not due to free polymer/reactants/solvent or other contaminants that are merely adsorbed onto the network surface during or after the polymerization.

To further confirm the presence of covalently attached polymer brushes, FTIR spectroscopy was used to characterize the composition of the polymer films before and after grafting. The FTIR spectra of the initial film collected in transmittance mode displayed peaks characteristic of a methacrylate network polymer, with the dominant peaks assigned to the carbonyl stretch (1725 cm⁻¹) and the C–H stretch (2950 cm⁻¹). After the network layer was subjected to surface polymerization conditions, new peaks were observed which corresponded to those expected for the corresponding polymer brush; for example, in the case of styrene new peaks were observed at 1602 and 3026 cm⁻¹ which correspond to the C=C and aryl C–H stretching bands for polystyrene.

The growth characteristics of the polymer brushes were examined by ellipsometry and the thickness changes of the polymer films related to the molecular weight of the grafted linear polymer chains (Table 2). In all cases the film thickness data supported the findings of the contact angle and FTIR measurements and the control sample, **PP1** containing no embedded inimer, showed no significant change in film thickness with a film thickness of 26 nm before and after polymerization. An increase in film thickness was observed for all of the inimer-doped films subjected to the polymerization conditions. The HEMA-grafted film showed the smallest increase of 13 nm after reaction, while the nitroxide-mediated polymerization had the largest change of 143 nm. Previous studies involving well-defined polymers grafted from initiators immobilized on solid surfaces in the presence of free initiator in the solvent phase have shown that the molecular weight of the polymer isolated from solution is a good approximation of the polymer grafted from the embedded inimers.¹⁸ In the case of the MMA and styrene ATRP polymerizations, the free polymer grown concurrently in solution was isolated and analyzed using GPC to determine the molecular weight and the molecular weight distribution. The low polydispersity (M_w/M_n) of the samples indicated that control of the polymerization, i.e., its “living” nature was preserved. To examine the nature of the relationship between observed film thickness and polymer molecular weight, a series of wafers with a thin film of **PP1** doped with 10 wt % inimer, **IN-1**, were reacted with styrene under ATRP in the presence of free initiator. The reactions were stopped at different times and the reaction solution, which contained nonsurface-attached or “free” polymer, was analyzed by GPC. The clean and dried wafer film thicknesses were measured and compared with the molecular weight of the free polymer formed in solution. As can be seen in Figure 3, a linear correlation between observed film thickness and polymer molecular weight with films ranging from 15 to 38 nm corresponding to molecular weights of 18–37 K, respectively.

The ability to employ embedded inimers and for those inimers to remain active after the contact-molding process now permitted growth from patterned features to be examined. The same contact-molding technique as described above was employed

(29) Jarvis, N. L.; Fox, R. B.; Zisman, W. A. In *Contact Angle, Wettability, and Adhesion*; ACS Advances in Chemistry Series 43; Fowkes, F. M., Ed.; American Chemical Society: Washington, DC, 1964.

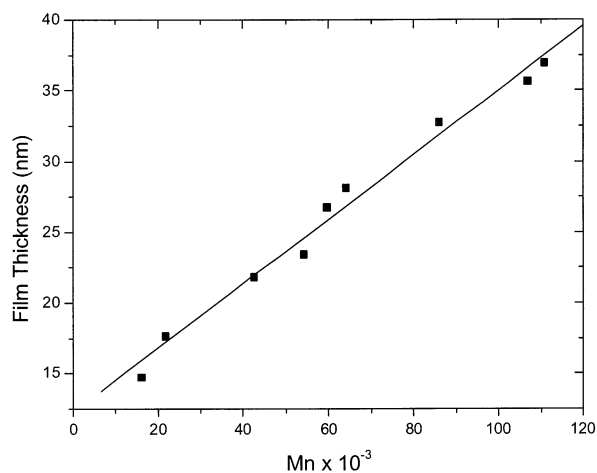


Figure 3. Molecular weight (M_n) vs thickness of surface ATRP polystyrene.

with a variety of patterned molds to replicate three-dimensional structures of inimer-embedded photopolymer. The resulting patterned polymer surfaces, containing embedded initiating sites, could then be used to initiate the grafting of well-defined polymer brushes.

These patterned films were subjected to the same surface polymerization conditions as described above for the flat surface studies with free initiator present in solution. After polymerization, the solution polymer was isolated and analyzed, and the molecular weights and molecular weight distribution were found to be similar to those observed for the flat surface samples, indicating that films of comparable thickness were grown on the surface of the patterned features when compared to flat surfaces. During the contact-molding process, it was not always possible to eliminate all traces of the photopolymer in the flat areas between the features where, ideally, full contact between mold and substrate is desired. To remove this thin, 1–3 nm layer of unwanted residue, a dry-etch process for its removal was examined, and again it was necessary to ensure that exposure of the inimer-embedded nanostructures to a harsh O_2 plasma etch would not destroy the initiating sites at the surface which are needed for subsequent polymerization. Test samples were prepared consisting of **IN-1**-doped **PP1** photopolymer and the films exposed to an O_2 plasma; both etch rates and chemical compatibility were then investigated. For **IN-1**-doped film having an initial thickness of 52.3 nm, etching for 30 s resulted in a decrease in the measured film thickness to 22.1 nm (ca. 10 Å/s). Significantly, reaction of the etched film under ATRP conditions with MMA gave behavior similar to that observed for nonetched films. In this case, the grafted PMMA layer was found to have a thickness of approximately 20 nm, and the M_n of the polymer grown in solution was 24 000 ($M_w/M_n = 1.27$). Similar behavior was observed for the alkoxyamine functionalized networks (**IN-2**), which indicates that these surface confined, living free radical initiators are stable to a wide range of conditions and processing steps.

To visualize the growth process and demonstrate the coupling of a top-down molding process with a bottom-up polymer brush growth process, patterned samples consisting of arrays of close packed pillars were prepared. The master used was manufactured by e-beam lithography and consists of rows of pillars with a 95-nm period, an average pillar width of 60 nm, and pillar-to-pillar separation of 35 nm.⁹ A mold was cast from the master,

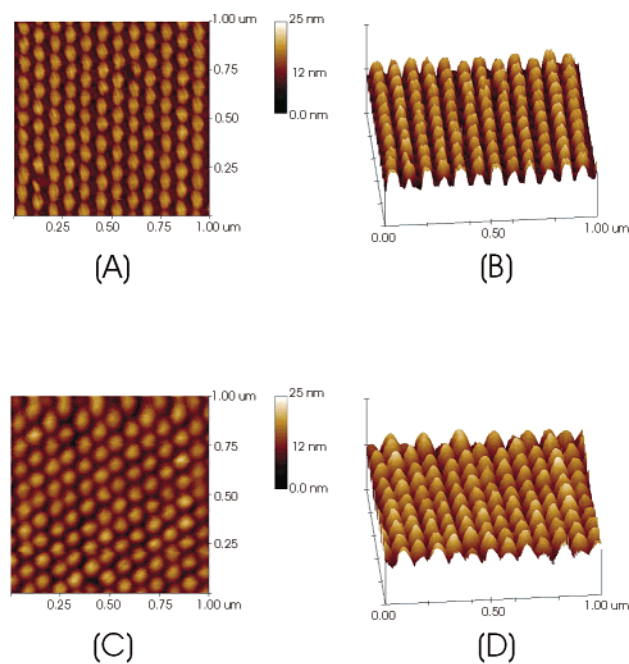


Figure 4. AFM of contact-molded pillars. (A) and (B) surface plots of the array of 60-nm pillars before polymer brush growth; (C) and (D) surface plots of the array of 75-nm pillars after brush growth.

as described above, and used to mold a thin layer of **IN-1**-doped **PP1**. Figure 4 shows an AFM image of the replicated pillars and demonstrates the excellent retention of the size and shape for the 60-nm pillars that can be achieved using this contact-molding procedure with the modified **PP1** formulation. The patterned substrate was then reacted with MMA for 4 h under ATRP conditions at 60 °C, and after thorough solvent extraction and drying, the modified nanostructures were examined by AFM. Interestingly, the pillars still had a 95-nm period; however, the size of the pillars was observed to increase from 60 to 75 nm with the interpillar spacing decreasing accordingly from 35 to 20 nm; this change of 15 nm is attributed to the growth of the polymer brush from the surface of the nanostructures.

To ensure that the nanoscopic size of patterned features could be controllably tuned, a series of ATRP reactions of MMA with varying molecular weights for the resulting PMMA chains were performed simultaneously on flat and patterned surfaces. The flat films were 30-nm thick films of **IN-1**-doped **PP1**, and the patterned surfaces consisted of molded **IN-1**-doped **PP1** with a repeating series of 100-nm wide lines. AFM and SEM images of identical areas of the patterned wafers are shown in Figure 5, A and B. The line edge roughness observed in the images was intentional and an artifact of the original masters made by e-beam lithography, the roughness being reproduced in succeeding daughter images. These intentional defects were employed as a means to determine the smallest size of features that could be reproduced and to give a range of feature sizes for subsequent growth from. In fact features as small as 5 nm have been faithfully reproduced by this patterning method.

The patterned and flat samples were then subjected to polymer brush formation by ATRP and the images in Figure 5, C and D, show the samples after grafting of the linear PMMA chains to the network structures. As can be observed, all of the features show an increase in size with the size increase being uniform

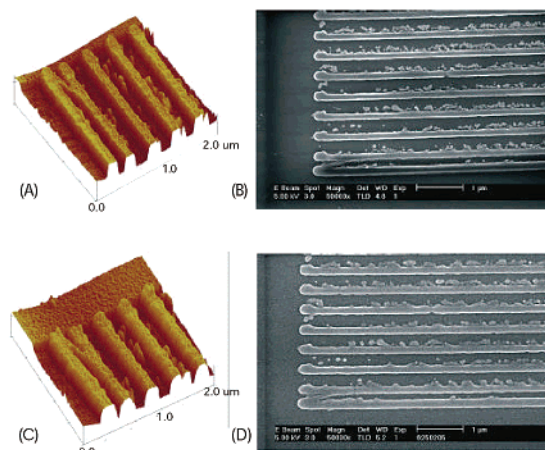


Figure 5. AFM and SEM images of contact-molded lines before (A), (B), and after ATRP brush growth (C), (D).

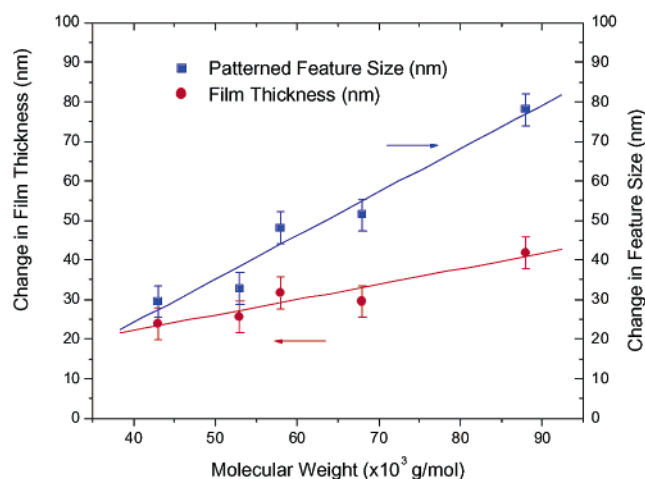


Figure 6. Demonstration of molecular weight and nanoscopic feature size control. Red line shows change in film thickness as a function of brush molecular weight. Blue line shows the change in molded feature width as a function of brush molecular weight.

regardless of the original feature size, which corresponds to a decrease in line-to-line separation.

The molecular weight of the polymer brush was varied from 43 to 88 K, and the resulting thickness changes of the flat films and the increase in line width for the patterned feature sizes are plotted in Figure 6. Again the correlation between molecular weight of the grafted chains and film/feature thickness change is excellent with a linear relationship in both cases. Of particular importance was the observation that the change in the line width was about double that of the corresponding flat films. This is

expected in the case of the lines since the thickness change results from uniform film growth on both sides of the features.

As a result the size of the nanoscopic lines can be controllably varied from their initial size of 100 nm to as large as 180 nm by simply varying the reaction conditions (sacrificial initiator, reaction time, monomer concentration). Since the period of the features does not change, a corresponding change in line spacing from 100 down to 20 nm is obtained. This combination of top-down and bottom-up techniques now provides a reproducible method for tuning feature sizes from a single master to suit lithographic requirements even to sub-50-nm features.

Conclusions

In summary, we have demonstrated the utility of combining a top-down contact-molding process with a bottom-up surface-initiating grafting strategy to form three-dimensional patterns in which the chemistry and size of the nanoscopic features can be accurately tuned. Pattern replication of features ranging from 5 μm to <60 nm can be achieved by contact molding a photopolymer mixture containing reactive inimers which lead to surface active sites for secondary polymerization. Both ATRP-type and nitroxide-mediated living free radical polymerizations can be initiated from the inimer-embedded surfaces leading to the formation of well-defined polymer brushes consisting of polystyrene, MMA, and HEMA linear chains. This leads to surfaces with different chemistries and physical properties. The grafts could be grown from either flat or nanopatterned substrates with controlled thickness ranging from 10 to 143 nm and with graft molecular weights estimated to range between 18 000 to 290 000 amu. The ability to control the growth of polymer brushes from contact-molded features can then be utilized to tune the size of nanoscopic features down to 20 nm. This novel combination of top-down and bottom-up strategies now gives researchers new tools for the reproducible fabrication of nanoscopic structures. Current work focuses on creating templates for pattern replication and the development of process steps for the transfer of these patterned images into a variety of substrates for patterned magnetic media and molecular electronics applications.

Acknowledgment. Financial support from the MRSEC Program of the National Science Foundation under Award Number DMR-9808677 for the Center for Polymeric Interfaces and Macromolecular Assemblies, and the IBM Corporation are gratefully acknowledged. Thanks to Teddie Magbitang for the GPC results and Justine Shaw for additional substrate preparation and processing.

JA028866N